INVESTIGATION OF URBAN ROCK VARNISH ON THE SANDSTONE OF THE SMITHSONIAN CASTLE

R.A. Livingston[1]*, C.A. Grissom[2], E.P. Vicenzi[3], Z.A. Weldon-Yochim[4], N.C. Little[5], J.G. Douglas[6], A.J. Fowler[7], C.M. Santelli[8], D.S. Macholdt[9], D.L. Ortiz-Montalvo[10] and S.S. Watson[11]

Abstract

Bluish black, highly adherent patches have been observed growing on the Seneca sandstone of the Smithsonian Castle in Washington, DC. They are enriched in Mn compared to the underlying sandstone, by a factor of 100, which suggests that microbial activity plays a role. The mineralogy is likely a mixture of birnessite and todorokite. Estimated thickness is on the order of 250 nm, 3 orders of magnitude thinner than typical desert varnish, and the patches lack the significant clay component found in desert varnish. However, the rate of growth, 9 nm/a, falls within the range of 1-40 nm/a measured for desert varnish. Trace amounts of Mn are found in Seneca sandstone, but they do not appear to be the major contributor to the varnish, which implies that airborne particulate matter would be a significant source. Ambient air concentrations of Mn have been measured at 4 ng/m^3 in the District of Columbia.

Keywords: manganese, varnish, Smithsonian Castle, elemental analysis, particulate matter

---

[1]*R.A. Livingston, Adjunct Professor, Materials Science and Engineering Department., U. of Maryland, USA, rliving1@umd.edu.

[2] C.A. Grissom, Senior Objects Conservator, Museum Conservation Institute (MCI), Smithsonian Institution, USA, grissomc@si.edu.

[3] E.P. Vicenzi, Research Scientist, MCI, vicenzie@si.edu.

[4] Z.A. Weldon-Yochim, Student, Art History Department, U. of Maryland, USA, zweldony@icloud.com.

[5] N.C. Little, Physical Scientist, MCI, littlen@si.edu.

[6] J.G. Douglas Head of Technical Studies, MCI, DouglJa@si.edu.

[7] A.J. Fowler, Research Fellow, Smithsonian National Museum of Natural History, USA, Alexandre.Fowler@gmail.com.

[8] C.M Santelli, Assistant Professor, Dept. of Earth Sciences, U. of Minnesota, USA, santelli@umn.edu.

[9] D.S. Macholdt, Graduate Student, Max Planck Institute for Chemistry, Germany, d.macholdt@mpic.de.

[10] D.L. Ortiz-Montalvo, Research Chemist, National Institute of Standards and Technology, USA, diana.ortiz-montalvo@nist.gov.

[11] S.S. Watson, Leader, Research Chemist, National Institute of Standards and Technology, USA, stephanie.watson@nist.gov.

*Corresponding author

1. Introduction

The Smithsonian Castle on the National Mall in Washington, DC, designed by James Renwick, Jr., was built in 1847-55. Figure 1 shows its distinctive Neo-Romanesque architecture constructed with dark red Seneca sandstone quarried in nearby Maryland (Livingston *et al.*, 2015). Gateposts made out of the sandstone according to Renwick's design were added in 1987 to enclose the Enid A. Haupt Garden.

Figure 1: South facade of the Smithsonian Castle and Enid A. Haupt Garden with the Gateposts in the foreground.

Figure 2: Patches of rock varnish on the southwest corner of the Smithsonian Castle.

Recently, visual inspection of the exterior of both the Castle and Gateposts identified patches of very thin adherent layers of bluish black material on the sandstone (see Fig. 2). Its distinctive appearance resembles desert varnish, which is thought to be associated with microbial action (Broecker and Liu, 2001). Nondestructive measurement of the set of patches in Figure 2 using portable X-ray fluorescence (pXRF) showed a high enrichment in manganese (Mn) (Livingston *et al.*, 2014a), which is also a sign of rock varnish. This has led to further research using an array of analytical techniques to characterize the varnish, the sandstone and the environment around the Castle (Table 1).

Table 1: Summary of analytical techniques

Topic	Methods
Varnish characterization	
Elemental composition	pXRF, LA-ICP-MS
Mineralogy	XRD, EPR
Thickness	SEM, hyperspectral XRF
Biology	DNA sequencing
Sandstone characterization	
Elemental composition	pXRF, INAA, PGAA
Microstructure	X-ray microanalysis
Varnish spatial distribution	Photogrammetry
Airborne particulate matter	High-volume air sampler

2 Varnish Characterization

2.1 Mn Enrichment

Nondestructive measurements made with pXRF at a number of points on the varnish as well as bare stone were used to calculate Mn enrichment. In order to compensate for variations in standoff, surface roughness, etc., results for locations on the Castle and a gatepost are reported as the ratio of the Mn peak to the adjacent Fe peak in Table 2. It can be seen that the ratios for the varnish are 50 to 100 times greater than the bare sandstone, indicating significant enrichment. The mean value for the Castle locations is roughly double that of the gatepost; this may be related to the greater age of the former, which would have provided more time to grow a thicker layer. On the other hand, the Mn/Fe for the bare stone is the same for both structures within experimental uncertainties, which indicates the uniformity of the underlying sandstone and is consistent with the ratio of 0.01-0.02 measured for the sandstone by instrumental neutron activation analysis (INAA) (Livingston *et al.*, 2015).

Table 2: Mn/Fe ratios measured by pXRF

Location	Varnish	Bare Stone
Castle	1.04 ± 0.5 (9)*	0.011 ± 0.02 (10)
Gatepost	0.55 ± 0.03 (5)	0.016 ± 0.003(5)

*Values in parentheses are number of data points

In addition to pXRF, laser ablation ion-coupled mass spectrometry (LA-ICP-MS) and X-ray microanalysis were applied to measure Mn and Fe on chips taken from the sandstone surface. The former method gave a mean Mn/Fe ratio of 4.1 and the latter, 4.5 ± 1.8 (Vicenzi *et al.*, 2016). Some of the differences are probably because of the inherent variability of the varnish, as shown by the large standard deviation for the Castle samples in Table 2. Also, the three methods sampled different patches. Finally, the sampled depth varied with the method and hence may have included more or less of the bulk sandstone. Nevertheless, the ratios all fall within a range of about 0.5-6.0, which is two orders of magnitude greater than the range of 0.01-0.02 in the bulk sandstone.

2.2 Mn Mineralogy

X-ray diffraction (XRD) of the varnish did not yield a usable diffractogram because of poor crystallinity or limited sensitivity given the sample thickness. An electron para-magnetic resonance (EPR) spectrum was obtained from a gatepost sample to constrain the chemical state of the Mn. This was compared to a set of standards of candidate Mn-bearing minerals including pyrolusite, manganite, lithiophorite, manganosite, birnessite and todorokite. Figure 3 presents a plot of the first derivative of absorption versus magnetic field strength for the Smithsonian sample compared to spectra of the most likely Mn minerals, birnessite and todorokite.

With X-ray microanalysis, it is possible to sample directly individual Mn-rich patches, as shown in Figure 4. The mean composition suggests a mixture of a Mn and silicate phase. Extrapolation to a Si-free end-member yields a composition consistent with birnessite (Fig. 5), which is the main Mn phase typically found in desert varnishes (Vicenzi *et al*., 2016).

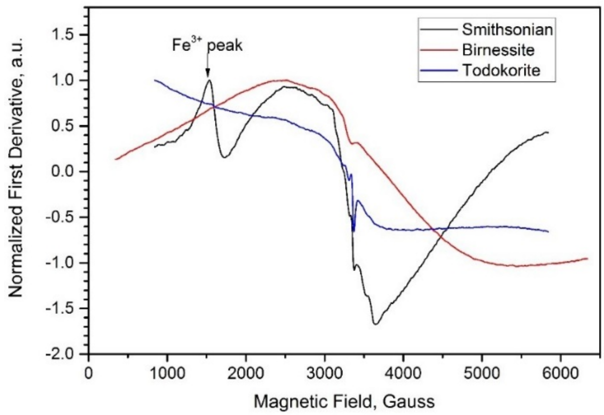

Figure 3: Comparison of the Smithsonian varnish EPR spectrum to Mn oxide mineral standards.

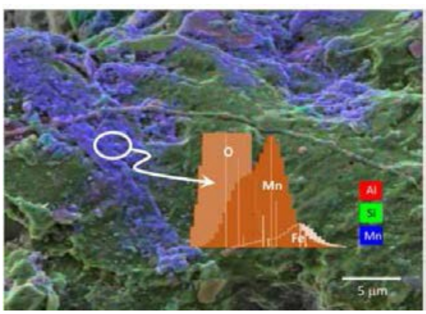

Figure 4: SEM image of a Mn-rich surface patch investigated by X-ray microanalysis. Mean composition:
$Na_{0.2}Ca_{0.1}Mg_{0.1}Al_{0.1}Si_{0.5}Mn_{1.9}Fe_{0.5}O_{6.7}$
(Vicenzi et al., 2016)

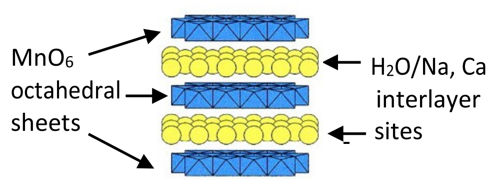

Figure 5: Birnessite structure:
$(Na,Ca)_{0.5}(Mn^{4+}, Mn^{3+})_2O_4 \cdot 1.5H_2O$
(Post, 1999).

2.3 Thickness

An SEM image of a cross-section of a chip taken from a gatepost is presented in Figure 6 overlain with an element map of Mn. It shows that the varnish layer is very thin and discontinuous on a microscopic scale on the surface and to a greater extent at depth along cracks and grain boundaries. Higher magnification images indicate that the varnish consists of fine particles of Mn between 20 to 200 nm in size. Unlike in desert varnish (see Fig. 7), clay minerals are largely absent in the layer.

An estimate of a nominal or effective varnish layer thickness of 250 nm was obtained from the X-ray microanalytical data (fig. 4) by modeling the attenuation of Si X-rays generated in the sandstone substrate by a layer of pure MnO_2 (Vicenzi *et al.*, 2016). This is three orders of magnitude smaller than the thicknesses of desert varnish layers. However, the rate of growth of the layer for the young age (28 years) of the Gateposts at 9 nm/a falls within the range of 1-40 nm/a measured for desert varnish.

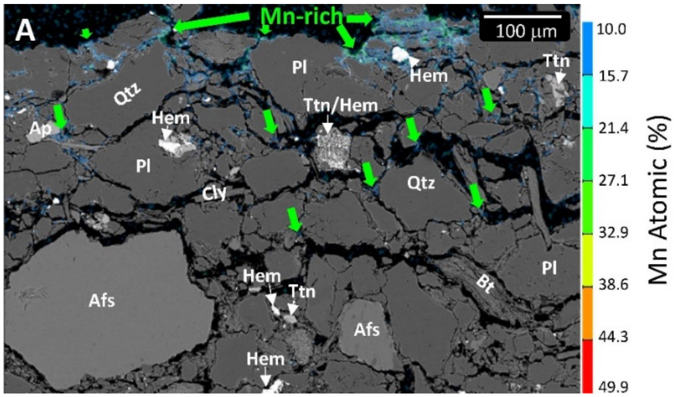

Figure 6: SEM image and elemental map of a polished cross-section of the varnish and sandstone from a gatepost (Vicenzi et al., 2016). Key: Afs =Alkali feldspar; Ap =Apatite; Bt =Biotite; Cly = Clay; Hem = Hematite; Pl = Plagioclase; Qtz = Quartz; Ttn = Titanite.

2.4 Biology

In order to determine the species of the Mn-oxidizing microbes responsible for growth of the varnish, swabs were taken at several locations on the Castle and Gateposts. The swabs were then applied to growth media on petri dishes to develop cultures. From these initial plates, active Mn-oxidizing microbes were isolated to produce the next generation of cultures. Figure 8 is an image of the end result of several generations of this isolation process

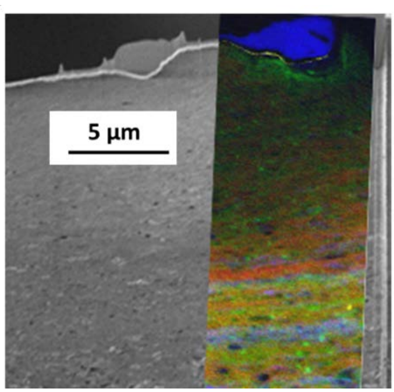

Figure 7: Optical (left) and (STXM) scanning transmission X-ray map (right) of desert varnish cross-section from the Mojave Desert in California (Macholdt et al., 2015). Key: red = Mn; green = Fe: blue = C; yellow = Ca.

for a swabbed patch on the southwest corner of the Castle shown in Figure 2. The colony has been identified as a fungus. The closest relative in the Genbank DNA database is *Leotiomycetes sp*. (accession #JQ761063.1). The identification as a fungus is consistent with SEM imaging of the varnish from the gatepost, which shows hyphae that are characteristic of fungal growth (Fig. 9).which shows hyphae that are characteristic of fungal growth (Fig. 9).

Figure 8: Colony of Mn-oxidizing fungus isolated from a Castle sample.

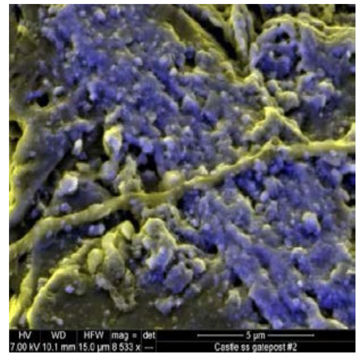

Figure 9:False colored SEM secondary electron (yellow)and backscattered (purple) image of possible fungal hyphae on surface of gatepost sample.

3. Sandstone Petrography

The Seneca sandstone used to build the Smithsonian Castle is formally known as the Poolesville Member of the Manassas Formation, which is in turn a member of the Newark Supergroup (Livingston *et al.*, 2015). The bulk chemical composition of the sandstone as determined by elemental analysis is given in Table 3. The elements were measured by INAA (Livingston *et al.*, 2014a), except for bound water, H_2O^+, which was measured by prompt gamma neutron activation (PGAA) (Livingston *et al.*, 2014b). Silicon was calculated by difference. The composition is consistent with the classification of the sandstone as arkosic and micaceous.

Table 3: Chemical composition of Seneca sandstone

SiO_2	Al_2O_3	CaO	MgO	Fe_2O_3	K_2O	Na_2O	TiO	MnO	H_2O^+
55.99	23.53	0.44	0.09	5.44	3.20	10.13	0.69	0.05	0.44

This composition is confirmed by the mineral assemblage identified in the SEM image in Figure 6. The most abundant detrital grains are quartz, plagioclase feldspar, alkali feldspar, and micas. Accessory minerals hematite (Fe_2O_3), titanite ($CaTiSiO_5$) and rutile (TiO_2) are present at minor to trace volumes. While these minerals typically contain minor Mn, the SEM-based compositional imaging reveals no pattern of Mn migration from these interior grains to the rock surface.

4 Airborne Particulate Matter

Since the source of Mn for the varnish does not appear to be the Seneca sandstone itself, another possibility is airborne particulate matter, either natural or anthropogenic. Analysis of twelve years of PM_{10} air pollution monitoring data from a District of Columbia-operated site located 3.38 km northeast from the Castle found an average ambient air concentration of roughly 4 ng/m^3. However, the site is relatively remote from heavy vehicular traffic, which may be a source of Mn. In contrast, the Castle is located next to a major roadway, Independence Avenue. Therefore, during the summer of 2015, an air pollution monitoring site was operated on the grounds of the Arthur M. Sackler Gallery of Art, located next to the Castle and Gateposts. This used a high-volume air sampler to collect particulate matter on 47 mm polycarbonate filters, which are now being analyzed.

5 Spatial Distribution of Varnish

In order to better understand the environmental factors influencing the development of the patches, their distribution was mapped by taking a comprehensive series of digital photographic images covering the entire building. Each identified patch was then manually mapped onto digital scale drawings of the elevations of the Castle using Adobe Photoshop, as illustrated in Figure 10. The area of each patch will be quantified, and the resulting data set will be used to investigate possible correlations with solar heating, prevailing wind direction, exposure to vehicular traffic, etc.

Figure 10: West elevation of the Castle modified from the Smithsonian's 2002 Master Plan Survey. Varnish patches are highlighted in red.

6 Conclusions

Elemental analysis of the varnish on the Castle and Gateposts has shown that it is significantly enriched in Mn compared to the underlying sandstone, by a factor of 100. This suggests that microbial activity may play a role. The mineralogy is likely a mixture of birnessite and todorokite, which is also consistent with microbial activity. The varnish thickness is estimated to be on the order of 250 nm, three orders of magnitude thinner than typical desert varnish; in addition, the varnish lacks a significant clay component found in desert varnish. However, the rate of growth of the layer is 9 nm/a, which falls within the range of 1-40 nm/a measured for desert varnish. The trace amounts of Mn in the Seneca sandstone do not appear to be the major contributor to the varnish, which implies that airborne particulate matter would be significant. Ambient air concentrations of Mn have been measured at 4 ng/m^3 in the District of Columbia, but they may be higher at the Castle because of its proximity to a major roadway. Future research includes obtaining more information on the biological aspects of the varnish; analyzing the ambient air concentration of Mn particulate matter; quantifying the distribution of the varnish around the Castle; and mapping the occurrence of the varnish on other sandstone structures in the Washington area.

7 Acknowledgements

Due to lack of space not all of the participants in this research could be listed as co- authors. These include: Emily Aloiz, Mohamad Al-Sheikhly, Elena Charola, Paula DePriest, Willa Freedman, Jennifer Giaccai, Klaus Jochum, Gwénaëlle Kavich, Robert Koestler, Florence Ling and John Ondov. The research has been supported by the Smithsonian's Museum Conservation Institute (MCI# 6453.2).

References

Broecker, W.S. and Liu, T., 2001, Rock varnish: Recorder of desert wetness? GSA Today 11(8), 4-10.

Livingston, R.A., Grissom, C. and Aloiz, E., 2015, Building stones of the National Mall, in Tripping from the Fall Line: Field Excursions for the GSA Annual Meeting, Baltimore, Brezinski, D.K., Halka, J.P., and Ortt, R.A., Jr. (eds.), Denver, CO, Geological Society of America, 40, 543–571.

Livingston, R.A., Grissom, C., Giaccai, J., Little, N., Vicenzi, E., Freedman, W. and Aloiz, E., 2014a, Dark crusts on urban sandstone: Natural or anthropogenic? in 2014 Goldschmidt Conference, Sacramento, CA, Geochemical Society, 1501.

Livingston, R.A., Al-Sheikhly, M., Grissom, C., Aloiz, E., and Paul, R., 2014b, Feasibility study of prompt gamma neutron activation for NDT measurement of moisture in stone and brick, 40th Annual Review of Progress in Quantitative NDE, Chiment, D.E., Bond, L.J. and Thompson, D.O. (eds.), American Institute of Physics, 1581, 828-835.

Macholdt, D.S., Jochum, K.P., Stoll, B., Pöhlker, C., Weis, U., Weber, B., Müller, M., Kappl, M., Buhre, S., Kilcoyne, A.L.D., Weigand, M., Scholz, D., Al-Amri, A.M., Andreae, M.O., 2015, Microanalytical methods for in-situ high-resolution analysis of rock varnish at the micrometer to nanometer scale, Chemical Geology 411, 57-68.

Post, J.E., 1999, Manganese oxide minerals: Crystal structures and economic and environmental significance, in Proceedings of the National Academy of Science, USA, 96, 3447-3454.

Vicenzi, E.P., Grissom, C.A., Livingston, R.A. and Weldon-Yochim, Z., 2016, Rock varnish on architectural sandstone: Microscopy and analysis of nanoscale manganese oxide deposits on the Smithsonian Castle, Washington, DC, Heritage Science, in press.